Analyst

Accepted Manuscript

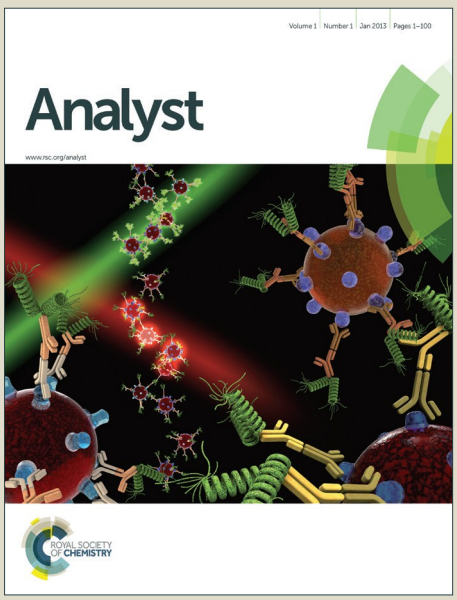

ROYAL SOCIETY OF CHEMISTRY

www.rsc.org/analyst

Analyst

RSCPublishing

PAPER

Nonlinear concentration gradients regulated by the width of channels for observation of half maximal inhibitory concentration (IC_{50}) of transporter proteins

Cite this: DOI: 10.1039/x0xx00000x

Received 00th January 2012,
Accepted 00th January 2012

DOI: 10.1039/x0xx00000x

www.rsc.org/

Yuta Abe,‡[a,c] Koki Kamiya,‡[a] Toshihisa Osaki,[a] Hirotaka Sasaki,[a] Ryuji Kawano,[a] Norihisa Miki[a,c] and Shoji Takeuchi*[a,b]

This paper describes a simple microfluidic device that can generate nonlinear concentration gradients. We changed the "width" of channels that can drastically shorten the total microfluidic channel length and simplify the microfluidic network design rather than the "length" of channels. The logarithmic concentration gradients generated by the device were in good agreement with those obtained by the simulation. Using this device, we evaluated a probable IC_{50} value of the ABC transporter proteins by the competitive transport assays at five different logarithmic concentrations.This probable IC_{50} value was in good agreement with an IC_{50} value (0.92 μM) obtained at the diluted concentrations of seven points.

Introduction

Determination of the half minimal inhibitory concentration (IC_{50}) of a drug is important to ascertain its safe and effective use. At this concentration, the binding or transport of the drug to membrane proteins is inhibited by 50% by another chemical substance *in vitro*.[1-3] Conventional IC_{50} measurement assays average the substrate transport in multiple cells and use batch-based procedures, such as microwell assays that require a serial dilution preparation of many kinds of the solutions by using a pipette and a large volume of sample.[4,5]

On the other hand, the use of a microfluidic concentration gradient device allows analysis of a high-throughput and a small sample volume; these devices enable us to rapidly investigate the dose dependency of the drug on one chip.[6,7] In particularly, a logarithmic concentration gradient generator is feasible for equal interval sampling of the drugs in a logarithmic scale,[8-11] compared to a linear concentration gradient generator.

One of the conventional microfluidic devices used for generating logarithmic concentration profiles is the pyramidal type, in which the microfluidic flow is repeatedly divided, mixed, and recombined through a microfluidic network.[12-14] The network can be used to produce complex concentration profiles by changing the relative flow rates, which is done by adjusting the length of the channels (the vertical channels), as shown in Fig. 1a. These devices have been applied for the analysis of cell culture and the conduction of chemotaxis studies.[13] The total length of the channel network increases with increasing number of outlets, which complicates the network design and makes the device more bulky. Tonner's group developed a simple universal concentration gradient generator; the "width" of the horizontal channels is used as the design parameter for achieving the desired flow divisions, rather than the "length" of the vertical channels at each branch.[15]

In this study, we propose a concept of flow division based on the width of horizontal channels for designing a nonlinear concentration gradient generator (Fig. 1b). This design would drastically shorten and simplify the microfluidic network compared to the conventional pyramidal designs. To design a device that is capable of producing five logarithmic concentration profiles, we first mathematically determine the width of the horizontal channel at each branch and adjust the flow rates of two inlets using simulation. We then examine whether the proposed device could generate logarithmic concentration profiles by using a fluorescent molecule. Finally, we perform dose-response assays using the ABC transporter proteins-reconstituted vesicles.[16]

Materials and method

2.1 Design

The design of the proposed device was based on adjustment of the width of the horizontal channels, and we verified the generated logarithmic concentration profiles using COMSOL Multiphysics simulation software. The channels in our nonlinear concentration device increased as $(1 + 2^{n-1})$ per branch (n: number of times of branch, number of outlets = 2, 3, 5, 9,…). We designed a nonlinear concentration device with five and nine outlets based on our concept (see Supplementary Design). Figure 2a and Supplementary Design shows a mathematical model of a microfluidic network that produces five logarithmic concentration profiles, namely, for 10^0 (=1.0), $10^{0.25}$ (=1.78), $10^{0.5}$ (=3.16), $10^{0.75}$ (=5.62), and 10^1 (=10). Two laminar fluids were injected into A0 (left) and E0 (right), where the concentration ratio was set at 10 to 1. The fluids from the upper vertical channels were divided at each branch and merged in the middle vertical channel (Fig. 2a). The ratio of the

flow division was determined by the geometry of the microfluidic channel-specifically the width of the horizontal channels. The width of the vertical channels was 100 μm. The length of the vertical channels was sufficiently long for mixing of two fluids by molecular diffusion (about 7.6 mm). The lengths of the horizontal channels at the first and second junctions were 200 and 100 μm, respectively.

2.2 Device fabrication and fluorescence measurement

The microfluidic devices were fabricated by standard photolithography and replica molding of PDMS.[17-19] Silicon wafer with patterned SU-8 negative photoresists (Nippon Kayaku, Tokyo, Japan) were used to form the master mold. The pre-cured PDMS (Sylgard 184, Dow Corning, Tokyo, Japan) was casted on the mold and baked at 75℃ for 90 min. The cured PDMS was then peeled off and punched to create the inlets and outlet. The height of the channels was 100 μm.

After preparation of the device, we confirmed the generation of the logarithmic concentration profiles using a fluorescence substrate. The device was immersed in a DI water pool, and removed air bubbles remained in the channels by degassing in a desiccator for 30 min. We then connected the syringes (Hamilton Company Japan, Tokyo, Japan) to the PEEK tubing (Grace, New York, USA), the inlets of which had inner and outer diameters of 0.1 and 0.5 mm, respectively. All the aqueous solutions were injected by mechanical micropumps (Hamilton Company Japan, Tokyo, Japan). 10 μM and 1 μM of a fluorescent substrate, rhodamine 123 (Rh123, Dojindo, Tokyo, Japan) were introduced into inlets A0 and E0, respectively. The initial flow rates through A0 and E0 were 0.8 and 1 μL/min, respectively. A fluorescence microscope (IX-71, Olympus, Tokyo, Japan) with an EMCCD camera (Andor Technology Ltd., Belfast, UK) was used to observe the concentration gradient generation of the Rh123 downstream.

2.3 MDR1 vesicles immobilization

Multidrug resistance protein 1 (MDR1), which is a member of ABC-transporter, was used in the experiment to determine the IC_{50}. To immobilize the MDR1 vesicles (GenoMembrane, Kanagawa, Japan) in the microchannels, we used the procedure of our previous work.[16] Single-stranded DNA (ssDNA, 5'-CAGTCAGTCAGTCAGTCAGTCAGTCAGTCAGTCAGTC AGT-3' BEX, Tokyo, Japan) was tethered to an aldehyde-coated glass slide and exposed to oxygen plasma for PDMS-glass bonding (FA-1, Samco, Kyoto, Japan). To prevent damage to the ssDNAs by the plasma exposure, we used a PDMS mask that covers the glass in which the ssDNAs were immobilized (Fig. S1a). After the plasma treatment, the PDMS-channel part was covalently bonded to the glass at 75°C for 30 min (Fig. S1b). Ten percent (v/v) fetal bovine serum (FBS) in PBS buffer (8.1 mM Na_2HPO_4, 1.5 mM KH_2PO_4, 137 mM NaCl, and 2.7 mM KCl at pH 7.4) was first introduced for 40 min to prevent undesirable absorption of the vesicles into the inner surface of the PDMS channels (Fig. S2b). After washing the channels with a 40 mM MOPS-Tris buffer (40 mM MOPS-Tris, 70 mM KCl, and 7.5 mM $MgCl_2$ at pH 7.0), a cholesterol-modified ssDNA (cholesterol-5'-ACTGACTGACTGACTGA CTGACTGACTGACTGACTG-3' (200 μL of a 1.43 μM in buffer, BEX)), which is complementary to the patterned ssDNA on the glass surface, was injected (Fig. S2c). After 45 min incubation to allow the formation of the DNA duplex, the channels were washed using a MOPS-Tris buffer. The MDR1 vesicles (200 μL of a 1 mg/ml MOPS-Tris buffer) were then injected and immobilized in the ssDNA-patterned area by means of the cholesterol, which acted as a membrane anchor (Fig. S2d). The flow rates during the procedure above were 10 μL/min. The syringe pump was stopped during the incubations.

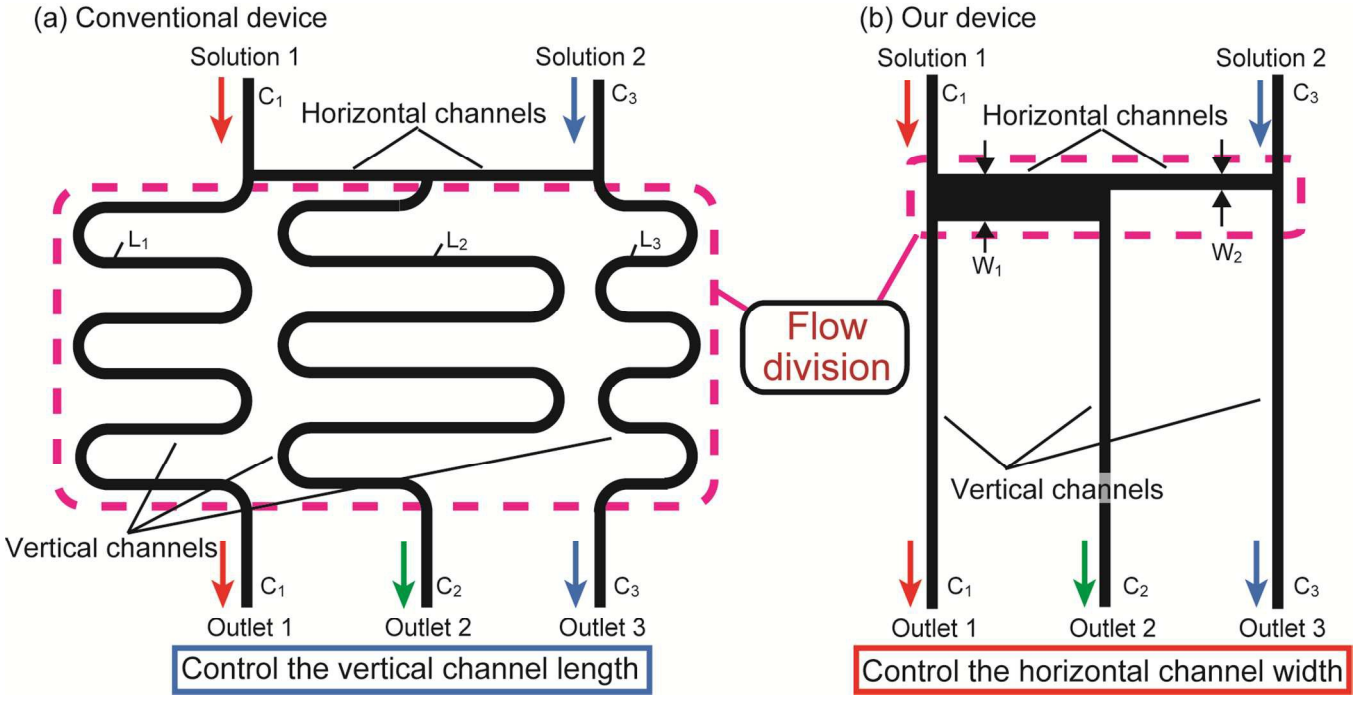

Fig. 1 Conceptual illustration of (a) conventional and (b) proposed device for producing logarithmic concentration profiles. The flow distribution ratios used for the arbitral concentration profile generation are controlled by (a) the vertical channel length and (b) the horizontal channel width.

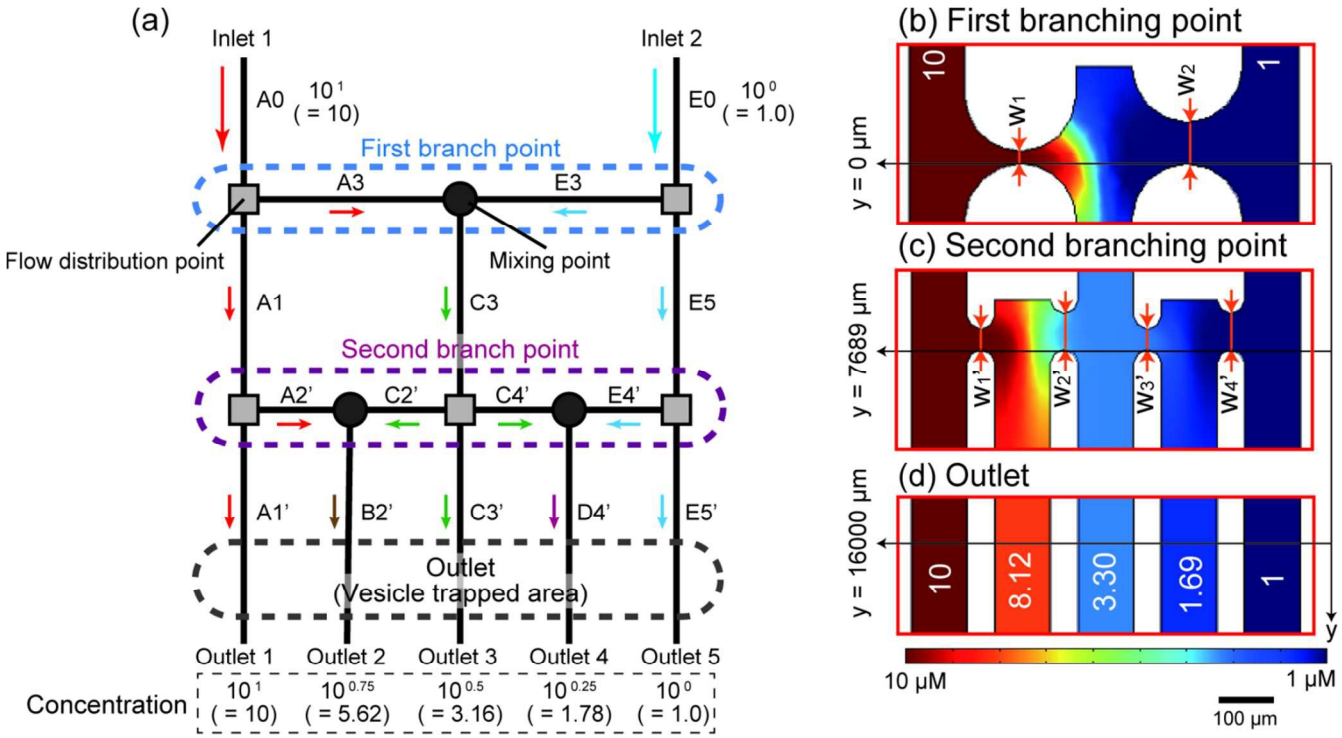

Fig. 2 (a) Schematic illustration of the microfluidic network. The square points indicate where the microfluids are divided and the circular points where the two microfluids are mixed. (b–d) Concentration generated at the branching points and outlets for hydrodynamic simulation. Scale bar: 100 μm.

2.4 Substrate transport of MDR1 along logarithmic concentration gradient

The substrate transportation by MDR1 was examined after the immobilization of the MDR1 vesicles. Solutions containing 10 mM ATP were injected into inlets A0 and E0 (see Fig. 2a) in the presence of either 1.0 or 0.1 μM Rh123, an MDR1 substrate. The flow rates through A0 and E0 were 0.16 and 0.2 μL/min, respectively. Supplementary Figures S3a-c show the three steps of the Rh123 transports: (i) The Rh123 and ATP solutions were introduced into the device (Fig. S3a); (ii) The MDR1 vesicles were incubated for 1 h, and the Rh123 molecules were transported by MDR1 (Fig. S3b); and (iii) The MDR1 vesicles in each channel were observed by fluorescence microscopy after washing using a buffer solution (Fig. S3c).

2.5 Competitive transport assay to determine IC_{50} values

Competitive transport assay for MDR1 was demonstrated with the proposed logarithmic gradient generator. We prepared the solutions by dissolving 50 nM Rh123 and 10 mM ATP in a MOPS-Tris buffer, using either 0.3 or 3.0 μM quinidine as an inhibitor. The solution containing 3.0 μM quinidine (high concentration) was injected into A0 at 0.8 μL/min, and that containing 0.3μM quinidine (low concentration) was injected into E0 at 1.0 μL/min. By this means, we are able to keep the concentrations of Rh123 and ATP constant while generating logarithmic concentration profiles for the quinidine. After incubation for 1 h at 37°C, we washed the channels using a MOPS-Tris buffer in the presence of a 50 nM Rh123 solution. The washing was done for 15 min using a flow rate of 10 μl/min. The intensities of the fluorescence of Rh123 in the MDR1 vesicles were analyzed by fluorescent images captured by a confocal microscope (TCS SP5, Leica Microsystems, Tokyo, Japan), and the mean values were calculated for each channel. The inhibition of the Rh123 transport was exhibited as the fluorescence intensity in the MDR1 vesicles. The data set of the substrate transport for different concentrations was normalized and fitted using equation (1)[16] for a dose-response

Table 1 Design parameters determined by hydrodynamic simulation for the generation of logarithmic concentration.

Inlet		A0	E0
Concentration	C (μM)	10	1
Flow rate	Q (μL/min)	0.8	1
Channel length	L (μm)	10000	10000
Channel width	W (μm)	100	100

1st junction		A1	A3	C3	E3	E5
Concentration	C (μM)	10	10	3.25	1	1
Flow rate	Q (μL/min)	0.61	0.12	0.59	0.42	0.60
Channel length	L (μm)	7653	200	7625, 7653	200	7625
Channel width	W (μm)	100	36	100	92	100

2nd junction & outlet		A1'	A2'	B2'	C2'	C3'	C4'	D4'	E4'	E5'
Concentration	C (μM)	10	10	8.12	3.25	3.30	3.25	1.69	1	1
Flow rate	Q (μL/min)	0.38	0.23	0.36	0.13	0.36	0.11	0.35	0.25	0.36
Channel length	L (μm)	10025	50	10025	50	10025	50	10025	50	10025
Channel width	W (μm)	100	36	100	64	100	36	100	64	100

curve (OriginPro 8.5J).

$$y = A1 + \frac{A2 - A1}{1 + 10^{(\log IC_{50} - \log x)p}} \quad (1)$$

where *A1* is the bottom asymptote, *A2* is the top asymptote, *x* is the applied inhibitor concentration, *y* is the fluorescence intensity, and *p* is the Hill slope.

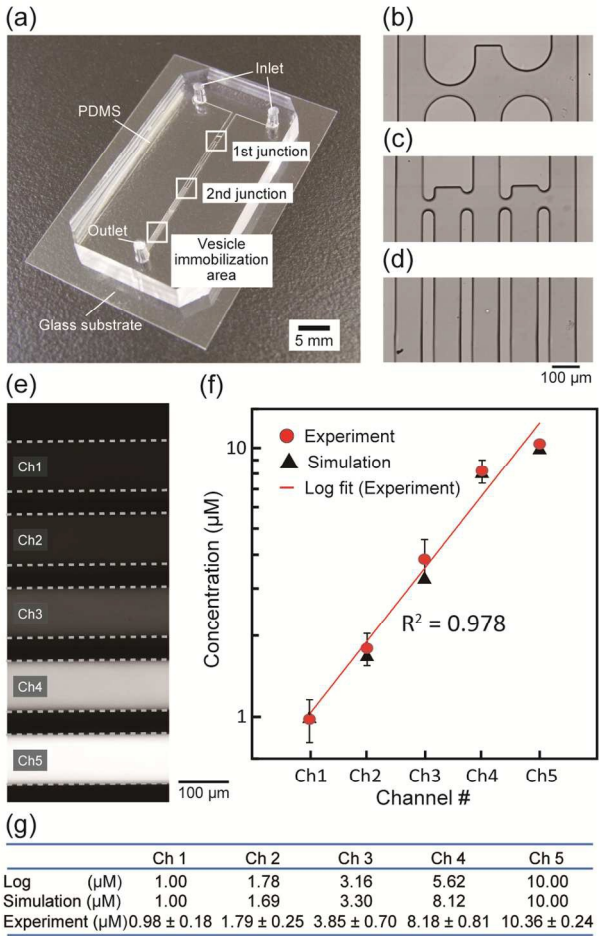

	Ch 1	Ch 2	Ch 3	Ch 4	Ch 5
Log (μM)	1.00	1.78	3.16	5.62	10.00
Simulation (μM)	1.00	1.69	3.30	8.12	10.00
Experiment (μM)	0.98 ± 0.18	1.79 ± 0.25	3.85 ± 0.70	8.18 ± 0.81	10.36 ± 0.24

Fig. 3 (a) A photograph of the logarithmic concentration generator. Microscopic images of (b) 1st junction, (c) 2nd junction, and (d) outlet. Scale bar represents 100 μm. (e) Fluorescence image of Rh123 in the logarithmic concentration generator. (f) This graph shows the concentrations calculated from the fluorescence intensity. Error bars indicate the standard deviation in each channel (N=2). The figures show the average concentrations at each channel by experiments. Black dots represent the concentration simulated by hydrodynamic simulation. (g) Comparison table of the concentrations with desires value, simulation, and experiment.

Results and discussion

3.1 Logarithmic fluid flow division at a horizontal channel

Figure 2b–d show the simulation results for the first and second junctions and the outlets. We found that the nearly logarithmic concentration profiles were generated when the width of the horizontal channels were 36, 92, 26, 64, 36, and 64 μm for A3, E3, A2′, C2′, C4′, and E4′, respectively. The generated concentrations for each channel were 10, 8.12, 3.30, 1.69, and 1. The initial flow rates through A0 and E0 were 0.8 and 1 μL/min, respectively. The dimensions, concentrations, and flow rates for each microchannel are given in Table 1. A logarithmic concentration generator was fabricated using these values. The total length of the channels in our device was about seven times shorter than that in conventional nonlinear concentration gradient device.[11] A logarithmic concentration gradient generator with nine outlets was also designed based on our concept. The concentration profiles of the simulated results nearly became logarithmic gradients at the nine outlets (Fig. S4), showing the scalability of our designing strategy.

3.2 Generation of logarithmic concentration gradient

We first confirmed the feasibility of logarithmic flow divisions in the developed device. Figure 3a is a photograph of the device and Figures 3b–d are microscopic images of the first and second branching points and the outlet. The concentration gradient generated in the device was evaluated from the fluorescence intensities obtained from the fluorescent microscopic images (Fig. 3e), and its calibration curve (Fig. S5). Figure 3f shows the graph of the generated logarithmic concentration gradients. The experimental values for outlet channels 1, 2, 3, 4, and 5 were 0.98±0.18, 1.79±0.25, 3.85±0.70, 8.18±0.81, and 10.36±0.24 μM (mean±s.d.), respectively. The desired, simulation, and experimental concentrations are compared in Fig. 3g. As can be seen, the logarithmic concentration gradients generated by the device were in good agreement with those obtained by the simulation except for the channel 4; this difference at channel 4 may be solved by increasing the width of channel C2' (see Fig. 2(a)) to increase the influx of the solution from channel C3 (see Fig. 2(a)).

3.3 Transport assays on MDR1 transporter

The potential of the logarithmic concentration generator developed was tested by transport assays using an ABC transporter. Rh123 was used as the fluorescent substrate of MDR1 to evaluate the transportation activities.[16] Figure 4 shows the fluorescence intensity in the MDR1 vesicles in each logarithmic channel. The insets show typical bright-field/fluorescence microscopic images of the trapped MDR1

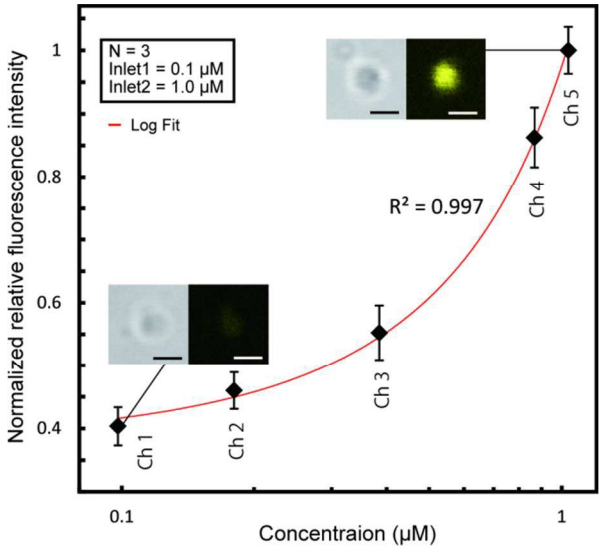

Fig. 4 Fluorescence intensities of the ABC-transporter vesicles after incubation for five different concentrations of Rh123. The bright field (left) and fluorescence (right) images of the vesicles after incubation are shown as insets. Scale bar: 1 μm. The error bars indicate the standard deviation. The fluorescence intensity generated in the vesicles increased proportionally with the Rh123 concentration.

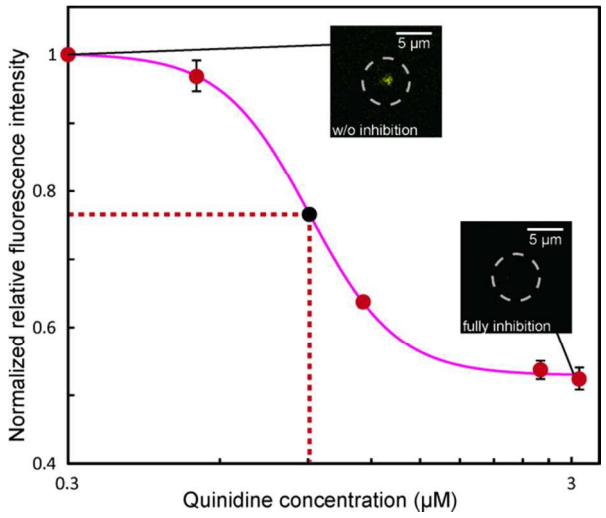

Fig. 5 Rh123 transport inhibition curves for quinidine. The curves were fitted to the experimental values obtained by logarithmic concentration generators.

vesicles at 0.1 and 1 μM Rh123, respectively. The fluorescence intensity of the vesicle loaded with 1 μM Rh123 was much higher than that of the vesicle loaded with 0.1 μM Rh123. The average fluorescence intensities after the transport assays were respectively obtained from approximately 30 single vesicles at each Rh123 concentration. The plot was closely fitted to the exponent curve, with the correlation coefficient (R^2) of 0.997 for a one-fold logarithmic concentration distribution, as shown in Fig. 4. This result is consistent with the former reports that the transport of Rh123 substrate into the MDR1 vesicles was linearly increased with the increase of substrate concentration.[16]

We then performed dose-response inhibition tests of Rh123 transport into vesicles using two devices, namely, the logarithmic concentration generator developed and a standard linear concentration generator (Fig. S6). The dose-response curves were obtained from the fluorescence intensities in each device. Figure 5 shows the experimental values, which represent the inhibition curves for quinidine (inhibitor of MDR1); the values were obtained at the five concentrations generated by each device. The y-axis represents the normalized fluorescence intensity; the fluorescence intensity was set to 1 for a quinidine concentration of 0.3 μM. The inset fluorescent microscopic images show the inhibitions of Rh123 influx into the MDR1 vesicles by 0.3 (left) and 3.0 μM (right) quinidine, respectively. The resulting IC_{50} for quinidine was 0.91±0.04 (mean±s.d.) (N = 3, n > 10) (Fig. 5). This IC_{50} value was in good agreement with an IC_{50} value (0.92 μM) obtained at the diluted concentrations of seven points using the linear concentration generator (Fig. S7).

Conclusions

We presented a design concept of the simple nonlinear concentration gradient device, which was based on a theory of changing the width of the horizontal channels. Our approach significantly shortened the total length of the microfluidic channels and simplified the microfluidic network design. The design is scalable and thus applicable to fabricate the generator with a large number of outlets as well as 2–3 ordered nonlinear concentrations. Therefore, we believe that the device would not only accelerate drug screening of transporter proteins, but also facilitate optimization studies in the various research fields including pharmacology, biochemistry, and analytical chemistry, where logarithmic scales are utilized.

Acknowledgements

We thank Utae Nose, Yoshimi Komaki and Maiko Uchida for technical assistance in the device preparation. This work was partly supported by the Regional Innovation Strategy Support Program of MEXT, Japan.

Notes and references

[a] Kanagawa Academy of Science and Technology (KAST), KSP EAST 303, 3-2-1, Sakado, Takatsu-ku, Kawasaki, Kanagawa, Japan. E-mail: takeuchi@iis.u-tokyo.ac.jp; Fax: +81-44-819-2092; Tel: +81-44-819-2037

[b] IIS, The University of Tokyo, 4-6-1 Komaba, Meguro-ku, Tokyo, Japan. Fax: +81-3-5452-6649; Tel: +81-3-5452-6650

[c] Keio University, 3-14-1, Hiyoshi, Kohoku-ku, Yokohama, Kanagawa, Japan. Fax: +81-45-566-1495; Tel: +81-45-566-1430

† Electronic Supplementary Information (ESI) available. See DOI: 10.1039/b000000x/

‡ These authors contributed equally to the work.

1 J. Rautio, J. E. Humphreys, L. O. Webster, A. Balakrishnan, J. P. Keogh, J. R. Kunta, C. J. Serabjit-Singh and J. W. Polli, *DMD*, 2006, **34**, 786.

2 K. M. Giacomini, S.-M. Huang, D. J. Tweedie, L. Z. Benet, K. L. R. Brouwer, X. Chu, A. Dahlin, R. Evers, V. Fischer, K. M. Hillgren, K. A. Hoffmaster, T. Ishikawa, D. Keppler, R. B. Kim, C. A. Lee, M. Niemi, J. W. Polli, Y. Sugiyama, P. W. Swaan, J. A. Ware, S. H. Wright, S. W. Yee, M. J. Zamek-Gliszczynski and L. Zhang, *Nat. Rev. Drug Discovery*, 2010, **9**, 215.

3 M. Gottesman and S. V. Ambudkar, *J. Bioenerg. Biomembr*., 2001, **33**, 453.

4 J. A. Cook, B. Feng, K. S. Fenner, S. Kempshall, R. Liu, C. Rptter, D. A. Troutman, M. Ullah and C. A. Lee, *Mol. Pharmaceutics*, 2010, 7, 398.

5 Y. Zhou, J. Yu, X. Lei, J. Wu, Q. Niu, Y. Zhang, H. Liu, P. Christen, H. Gehring and F. Wu, *Chem. Commun*., 2013, 49, 11782.

6 J. Pihl, J. Sinclair, E. Sahlin, M. Karlsson, F. Petterson, J. Olofsson and O. Orwar, *Anal. Chem*., 2005, **77**, 3897.

7 D. Lombardi and P. S. Dittrich, *Expert Opin. Drug Discov*., 2010, **5**, 1081.

8 K. Lee, C. Kim, Y. Kim, K. Jung, B. Ahn, J. Y. Kang, K. W. Oh, *Biomed. Microdevices*, 2010, **12**, 297-309.

9 C. Chen, A. M. Wo and D. Jong, *Lab Chip*, 2012, **12**, 794.

10 C. Kim, K. Lee, J. H. Kim, K. S. Shin, K. Lee, T. S. Kim and J. Y. Kang, *Lab Chip*, 2008, **8**, 473.

11 K. Lee, C. Kim, B. Ahn, R. Panchapakesan, A. R. Full, L. Nordee, J. Y. Kang and K. W. Oh, *Lab Chip*, 2009, **9**, 709.

12 K. Campbell and A. Groisman, *Lab Chip*, 2007, **7**, 264.

13 T. Glawdel, C. Elbuken, L. E. J. Lee and C. L. Ren, *Lab Chip*, 2009, **9**, 3243.

14 D. Amarie, J. A. Glazier and S. C. Jacobson, *Anal. Chem*., 2007, **79**, 9471.

15 D. Irimia, D. A. Geba and M. Toner, *Anal. Chem.*, 2006, **78**, 3472.

16 H. Sasaki, R. Kawano, T. Osaki, K. Kamiya, and S. Takeuchi, *Lab Chip*, 2012, **12**, 702.
17 X. Jiang, J. M. K. Ng, A. D. Stroock, S. K. W. Dertinger and G. M. Whitesides, *J. Am. Chem. Soc*., 2003, **125**, 5294.
18 S. Hong, Q. Pan and L. P. Lee, *Integr. Biol.,* 2012, **4**, 374.
19 M. Hosokawa, T. Hayata, Y. Fukuda, A. Arakaki, T. Yoshino, T. Tanaka and T. Matsunaga, *Anal. Chem*., 2010, **82**, 6629.

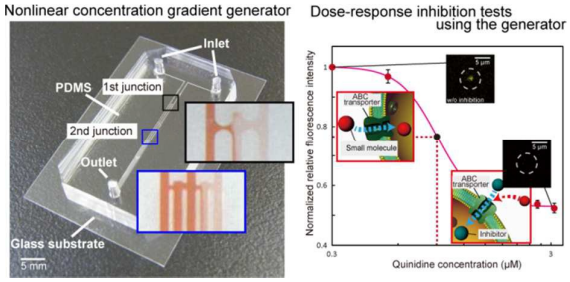

We determine a probable IC_{50} value of ABC transporter proteins by using a width-modulated nonlinear concentration gradient generator.